Highlights of Spanish Astrophysics XI, Proceedings of the XV Scientific Meeting of the Spanish Astronomical Society held on September 4–9, 2022, in La Laguna, Spain. M. Manteiga, L. Bellot, P. Benavidez, A. de Lorenzo-Cáceres, M. A. Fuente, M. J. Martínez, M. Vázquez- Acosta, C. Dafonte (eds.), 2023

Formation of ring-like structures in flared α-discs with X-ray/FUV photoevaporation.

Vallejo, Juan C.[1,2], and Gómez de Castro, Ana I.[1,2]

[1] AEGORA research group - Joint Center for Ultraviolet Astronomy, Universidad Complutense de Madrid, Plaza de Ciencias 3, 28040, Madrid, Spain
[2] Departamento de Física de la Tierra y Astrofísica, Fac. de CC. Matemáticas, Plaza de Ciencias 3, 28040 Madrid, Spain

Abstract

Understanding the evolution of protoplanetary discs is key to understand the formation of planets around young stars. However, modelling these protoplanetary discs is not an easy task as several complex dynamical processes must be included in the numerical models. In this work, we analyse the impact of adding a progressive flattening in protoplanetary flared discs combined with different photoevaporative winds in the creation of ring-like structures, using a simple semi-analytical 1D α-disc. Our results show that such a progressive flattening may favour the formation of ring-like features resembling those observed in real systems. Depending on the control parameters, these features are created with proper disc masses and accretion rates at the right evolutionary times. However, further enhancements are still needed for better matching all the evolutionary times seen in real systems.

1 Introduction

The protoplanetary discs are the natural scenario for planet formation processes. Analysing their dispersal time-scales constraint the time in which those planets must form, while computing their masses at given times provide the mass available for planet formation.

We will focus here on modelling the so-called transitional discs. These discs have relatively short-lived inner cavities and gaps. Hence, analysing their creation and lifetimes will help in refining the model parameters.

Because of the complexity of the problem, we take an approach based on a semi-analytical 1D viscous α-disc, with a flaring profile that changes with time added to a photoevaporative term.

Viscous momentum transport is of interest in disc modelling from disc-possessing to discless status even when other transport alternatives are possible. In principle, the molecular viscosity of the gas is too small to produce significant evolution. Despite of above, a viscous approach is still quite common when ones interprets the viscosity as the outcome of a turbulent process.

Hence, the surface density $\Sigma(r,t)$ evolves as per the laws of mass and momentum conservation, with a diffusion coefficient regulated by the viscosity ν as follows,

$$\frac{\partial \Sigma}{\partial t} = \frac{3}{r}\frac{\partial}{\partial r}[r^{1/2}\frac{\partial}{\partial r}(\nu \Sigma r^{1/2})] - \dot{\Sigma}_w, \tag{1}$$

where $\dot{\Sigma}_w$ denotes the mass loss by a given photoevaporative wind, functionally equivalent to have a sink in this diffusion equation.

The photoevaporation can explain the two time-scales behavior observed in real systems, the shutdown of the mass accretion and disc dispersion at proper time scales. And an inside-out dispersal model produced by photoevaporation can naturally produce the observed internal cavities and gaps in the disc,

This can be considered a may be too simple model. There is not magnetic field, envelopes or other 2D/3D structures. Moreover, it does not include hydrodynamics, chemical processes, radiative or MHD processes. Many of these different mechanisms could create the observed ring-like features.

Despite of this, simple 1D (semi-)analytical models are still in use nowadays. They complement more complex models meanwhile offer simplicity in interpreting the results. And, because they can incorporate further details in a bottom up approach, they are ideally suited for the α-parametrization and numerical winds.

We extend the initial analyses carried out in [14], and we will evolve a set of models corresponding to a grid of physically meaningful systems covering some of the typical parameter values. Among all possible parameters, we will focus on those defining the disc (disc mass, host star mass, accretion rate, disc age), viscosity values, the time scales when the progressive flattening of the flared disc takes place and the different efficiencies of the photoevaporative winds.

The final goal will be to crosscheck the results with the ring-like features observed in some reference real systems located in the Taurus star forming region, aiming to see how different parameter affect their creation.

2 The numerical α-discs

The α-parametrisation was firstly introduced as a convenient scaling factor of the friction between adjacent rings. This parametrisation was firstly used in [12] and later refined in [13]. It hides the details of the specific viscous transport mechanism while reflecting the impact of the transport in the disc evolution. Therefore, as this parametrisation simplifies the implementation of the viscosity in numerical models, it has been widely used for many years and it is still in common use today [8, 9, 2].

This model relies on an optically thick accretion disc and a turbulent fluid described by a viscous stress tensor, with this stress tensor being proportional to the total pressure. When the eddy size (mean free-path) is less than the disc height and the turbulent velocity smaller than the sound speed c_s, one can write the viscous profile as $\nu(r) = \alpha c_s H(r)$, with $H(r)$ the scale height profile that models the disc thickness, presuming $H(r) << r$ for a thin disc.

Considering hydrostatic equilibrium perpendicular to the disc plane and a simple relationship between the disc and surface temperatures, the sound speed can be written as $c_s = H(r)\Omega$, with Ω is the circular keplerian velocity [7]. Hence, the ν viscosity at a given distance r depends on rotation, with a linear dependency on the mass of the star M_* and on the flaring of the disc,

$$\nu(r) = \alpha \frac{c_s^2}{\Omega} = \alpha \Omega H^2(r). \tag{2}$$

Note that Magneto Rotational Instability (MRI) was a widely used candidate for modelling turbulence and angular moment transport, but MRI can be suppressed by non-ideal MHD. Other mechanisms such as outflows, gravitational instabilities or magnetic winds can also play a fundamental role in the evolution of the disc, but they do not exclude the viscous transport.

So, α-parametrisation can be seen as a mere (re)parametrisation of the viscosity, but also as a value that models the whole disc reflecting the different effectiveness of the different hidden processes.

A value of $\alpha = 0.01$ was typically used because it usually provides evolutionary time-scales in line with known properties of discs [5, 4]. Later on, values ranging from $\alpha = 0.1$ to 0.001 have been also used [1, 3, 7]. Nowadays, even lower values $\alpha = 10^{-4}$ can be found [2, 10], and these seems to better agree the observed discs [14, 15].

3 The photoevaporative wind

A simple 1D model can incorporate different radiation fields and be at the same time a convenient way for exploring the role of the different parameters. The photoevaporative wind will be different depending on the different heating radiation mechanisms. These winds can be dominated by EUV radiation, with energies from 13.6 eV to 0.1 keV, capable of ionising an Hydrogen atom. But also by fields dominated by X-rays radiation, with photons of energies ranging from 0.1 keV up to $1-2$ keV. These much energetic photons can penetrate large hydrogen columns but provide small heatings. Finally, one can also consider winds dominated by FUV radiation, embracing energies from 6 eV to 13.6 eV, capable of dissociating the H_2 molecule.

As a consequence, the wind term physics can be very complex. However, it can be included on the model as a simple mass sink term in the density surface evolution equation, in the form of numerical fits to the results coming from more complex simulations (as those from [11], [7] or [6]). The profiles corresponding to these results can be seen in the Fig. 1.

3.1 The progressive flattening of the disc

The flaring profile is a key parameter that defines the sound speed c_s profile, and, in turn, the temperature profile of the disc. The temperature depends on the amount of stellar radiation

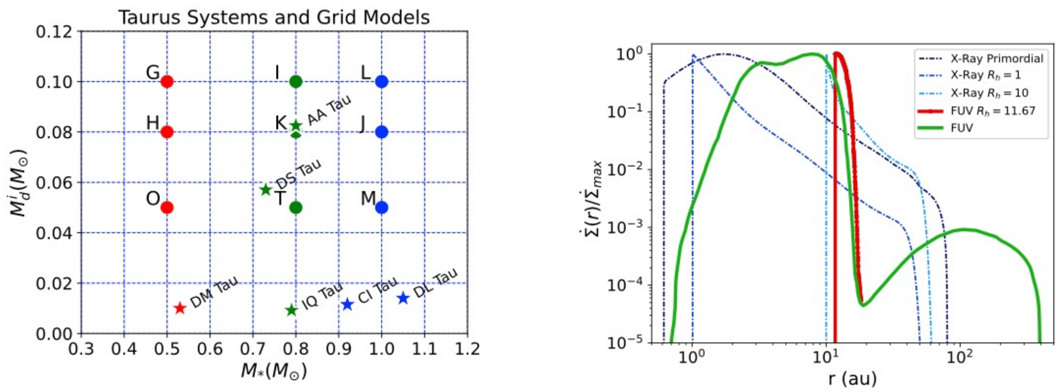

Figure 1: (left) The selected grid of discs models in the M_*–M_d^i plane. The initial disc masses M_d^i decrease as the discs evolve. Hence, these initial points move downwards in the diagram, approaching to the parameters observed in real Taurus systems. (right) Normalised photoevaporative wind mass losses corresponding to the FUV wind profiles described in [6] and the X-ray wind profiles from [11].

impacting the disc, which also rests on its geometry again. Hence, the resulting scale height $H(r)$ can follow an approximate power law dependence,

$$H(r) = \kappa\, r^h. \tag{3}$$

Even when it is customary to keep constant the flaring profile of the disc, it seems reasonable to consider that this flaring may change with time, with a progressive flattening of the disc as the age increases. Therefore, we will include in our simulations a changing profile for the flared disc, by decreasing the κ parameter in Equation 3 at given times.

4 Results

We have solved the evolution of the surface density derived from Equation 1, for different stellar masses and disc masses. We can observe in Fig. 2 that some features resembling the observed ring-like structures can be obtained with our simple photoevaporative models.

Further details and results can be seen in [15]. A progressive flattening of the disc seems to support the production of ring-like features at the observed ages. For certain viscosities, discs with large gaps and strong accretion rates, which have been linked to giant planet formation, can be also obtained.

However, our simple models do not reproduce in full all reference real systems. The produced features seem to be short-lived and some additional mechanism may be needed for carving faster the dents and create real gaps with proper lifetimes. This points to add further flattening laws and new winds evolution in a broader grid, and may be to extend the available wind efficiencies.

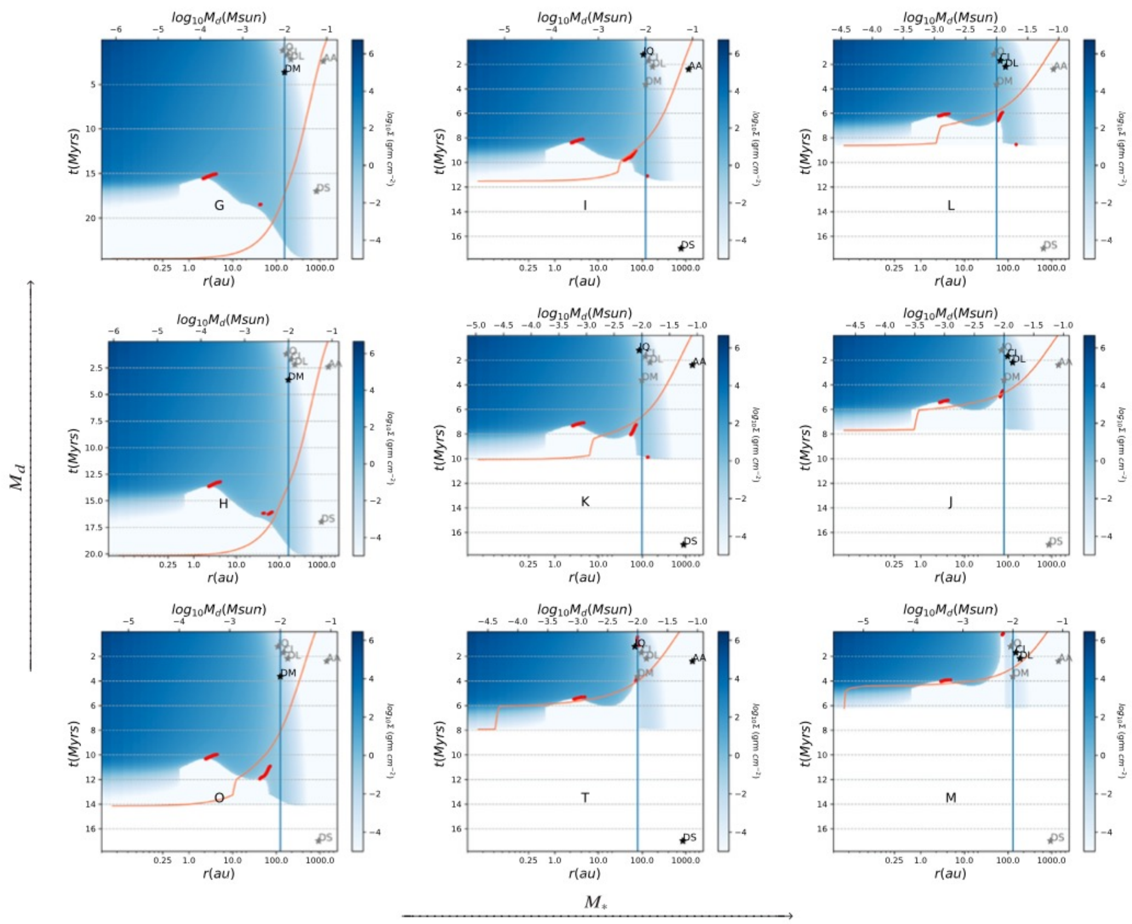

Figure 2: Evolution of the grid of models for a fiducial photoevaporation controlled by X-ray heating, efficiency factor=1.0, a viscosity value of $\alpha = 10^{-4}$ and a progressively flattened flaring profile. The surface density in blue gets lighter as the disc is eroded. The red points indicate local minima in the density profiles. The second dent can be carved at the same time or even at earlier times than the the inner dent. These two dents can produce ring-like features when exist at the same time. Sometimes, these two dents can be accompanied by a third outer dent. Some Taurus discs are also plotted for reference. They appear in black when their stellar masses are similar to the mass of the analysed synthetic model. Otherwise, they appear in grey.

Acknowledgments

The authors thank the Spanish Ministry of Economy, Industry and Competitiveness for grants ESP2015-68908-R and ESP2017-87813-R.

References

[1] Andrews, S.M., Wilner, D.J., Hughes, A.M., Qi, C., Dullemond, C.P., 2009, ApJ, 700, 1592.

[2] Ercolano, B., Jennings, J., Rosotti, G., Birnstiel, T., 2017, MNRAS, 472, 411.

[3] Gorti, U., Hollenbach, D., 2009, ApJ, 690, 1539.

[4] Hartmann L., Calvet, N., Gullbring, E., and D'Alessio, P., 1998, ApJ, 495, 385.

[5] Hawley, J.F., Balbus, S.A., 1995, PASA, 12, 159H.

[6] Jennings, J., Ercolano, B., and Rosotti, G.P., 2018, MNRAS, 477, 131.

[7] Jones, M.G., Pringle, J.E., Alexander, R.D., 2012, MNRAS, 419, 925.

[8] Kimura, S.S., Kunitomo, N., Takahashi, S.Z., 2016, MNRAS, 461, 2257.

[9] Lodato, G., Scardoni, Ch.E., Manara, C.F., Testi, L., 2017, MNRAS, 472, 4700.

[10] Martin R.G., Nixon, C.J., Pringle, J.E., Livio M., 2019, NewA, 70, 7M.

[11] Owen, J.E., Clarke, C.J. and Ercolano, B., 2012, MNRAS, 422, 1880.

[12] Shakura, N.I., Sundayev, R.A., 1973, A&A, 24, 337.

[13] Shakura, N.I., Sundayev, R.A., 1976, MNRAS, 175, 613.

[14] Vallejo, J.C., Gómez de Castro, A.I., 2018, APSS, 363, 246.

[15] Vallejo, J.C., Gómez de Castro, A.I., 2021, MNRAS, 508, 950.